International Journal of Technology 13(1) 157-167 (2022)
Received December 2020 / Revised July 2021 / Accepted August 2021

International Journal of Technology

http://ijtech.eng.ui.ac.id

Few-Layer Wrinkled Graphene (FLwG) Obtained from Coconut-Shell-Based Charcoal using a High-Voltage Plasma Method

Fri Murdiya[1], Yola Bertilsya Hendri[2], Amir Hamzah[1], Neni Frimayanti[3], Amun Amri[2*]

[1]*Department of Electrical Engineering, Universitas Riau, Kampus Binawidya Panam, Riau 28239, Indonesia*
[2]*Department of Chemical Engineering, Universitas Riau, Kampus Binawidya Panam, Riau 28239, Indonesia*
[3]*Department of Pharmacy, Riau College of Pharmacy (STIFAR), Jl. Kamboja Panam, Riau 28239, Indonesia*

Abstract. Few-layer wrinkled graphene (FLwG) has been synthesized from a coconut-shell-based charcoal using a high-voltage plasma method. Raman spectroscopy, transmission electron microscopy (TEM), and X-ray diffraction (XRD) were used for characterizations. Molecular dynamic simulation was also performed for further atomic/molecule movement analysis in the system. The plasma was supplied in the air gap between the electrodes. The graphite rod was used as the high voltage electrode and the aluminum plate was used as the co-electrode. The charcoal powder was arranged on the aluminum electrode surface in the air gap with a distance of ~3 cm to the graphite electrode. Raman spectroscopy analysis indicated that an FLwG had been produced. TEM analysis confirmed the presence of FLwG with a wrinkled and folded structure with an average size of 48.03 nm. XRD revealed that the produced graphene did not undergo any oxidations. Molecular dynamic simulation predicted that the FLwG formation was mainly led by the combination of ionization and deionization of air molecules under high temperatures and plasma stressing.

Keywords: Coconut-shell-based charcoal; Few layers wrinkled graphene; High voltage plasma; Resonance inverter

1. Introduction

Research on the manufacture of graphene with methods that are suitable for the large scale is currently widespread. Various methods have been used, such as exfoliating graphite using liquid shear exfoliation and sonication, and they are quite promising (Wall, 2011; Fatima et al., 2014; Arifutzzaman et al., 2019; Luong et al., 2020; Amri et al., 2021). However, the risk is significant due to the disposal of liquid waste, which is dangerous to the environment. A new approach to graphene synthesis on a large scale, without any disposal liquid, has been reported (Luong et al., 2020). Luong et al. (2020) found that the synthesis of graphene using impulse energy techniques from an electric charge in capacitor banks could reach temperatures higher than 3,000 K in the order of 100 ms. Furthermore, it was found that extreme temperatures affected the peeling of carbon materials to graphene under the release of impulse energy from capacitor banks (Cançado et al., 2008; Kaniyoor et al., 2010).

The use of the electric currents in the process of graphene production, however, is still not optimal (Luong et al., 2020). With the flash joule heating (FJH) process, the produced

*Corresponding author's email: amun.amri@eng.unri.ac.id, Tel.: +62-761-66596, Fax.: +62-761-66595
doi: 10.14716/ijtech.v13i1.4572

graphene was of better quality and could be used as a composite building material (Luong et al., 2020). This process required an increased compression of the powdered charcoal to reduce the electrical resistance, and it was necessary to maintain the temperature in the experiment around ~ 3,100 K in the order of 10 ms. This process produced graphene with a higher 2D band of Raman spectra. If the FJH flash exposure time was in the range of 50 to 150 ms, the produced graphene had a Raman spectra with a lower 2D value (Botas et al., 2013). The use of arc discharge in the manufacture of graphene has also been reported (Poorali and Bagheri-Mohagheghi, 2017). They arranged two electrodes made of graphite with ZnO and TiO_2 as catalysts and injected an AC power supply of 100-200 A into the system (Poorali and Bagheri-Mohagheghi, 2017).

In our previous work, we reported the use of a resonant inverters circuit for high-voltage ozone generators with a push full configuration (Fri et al., 2020). The ozone generator was arranged with a dielectric barrier discharge method. It was found that the life of electronic components was inadequate and that overcurrent protection was needed in the event of an increase in current due to the enlarging plasma. This circuit provided a voltage of up to 15 kV with a frequency of 25 kHz (Fri et al., 2020). The aim of this current work is to synthesize graphene from coconut-shell-based charcoal using a high-voltage plasma (arc discharge) method. The plasma was created by modifying a previous ozone generator circuit to produce a high voltage in the order of 8 kV and a frequency of 25 kHz. Its peak voltage was established to produce plasma that was different from the barrier discharge in the previous ozone generator. Through this method, few-layer wrinkled graphene (FLwG) was successfully produced. FLwG has high potential to be used in energy storage and supercapacitor applications with high surface areas, high conductivity, thermal stability, and mechanical and chemical robustness (Deng and Berry, 2016).

2. Methods

2.1. Materials and High-Voltage Plasma Circuit

The raw material used in this work was coconut-shell-based charcoal, which was crushed to form charcoal powder. It was then directly stressed by plasma arc discharge without any further special treatment. The implementation of resonant-inverter-generated high voltage ozone generators with a push full configuration has been reported. The complete electronic circuit of the resonance inverter is given in Figure 1. The inverter input voltage was supplied from a direct current power supply of 15 volts. The MOSFET firing circuit used an IC CD4047 that was a pulse width modulation (PWM) integrated circuit. Six MOSFETs (M_1...M_6) as semiconductor or static switches were connected parallel to form a bridge, and it was installed to 12 Vdc. This circuit was equipped with an inductor (L) of 10 mH and connected in series with a capacitor (C_2) of 150 nF. The resonant circuit's output was connected to a fly-back transformer's low-voltage side; the primary coil was a center tap with several turns 10/2. The fly-back transformer's high-voltage side was connected to a graphite rod and an aluminum plate electrode. The high-voltage resonant inverter generator was energized by an input voltage of 220 VAC and a frequency of 50 Hz. This inverter's output voltage can reach 8 kV under load conditions at a frequency of 20 kHz (Fri et al., 2020). The use of a microcontroller-based overcurrent protection device in electronic circuits aims to protect the equipment from heat when an increasing current occurs in static switching (MOSFET) due to the more massive plasma produced. With changing plasma volume, the protection device will monitor the increasing current so that the circuit breaker will automatically open from the source. The research applied a graphite electrode with a length of 10 cm and a diameter of 0.7 cm, which was different from previous findings. The electrode on the other side used an aluminum plate with dimensions of 20 cm × 20 cm × 3

mm in length, width, and thickness, respectively. The distance of the graphite electrode to the charcoal powder was ~3 cm. The light intensity of the arc discharge was recorded by an Aspectramini app on Android software. The discharge current and voltage were measured by a Hantek CC650 current probe and SEW voltage divider with a ratio of 1,000:1. This discharge current and voltage were recorded by a Hantek digital oscilloscope.

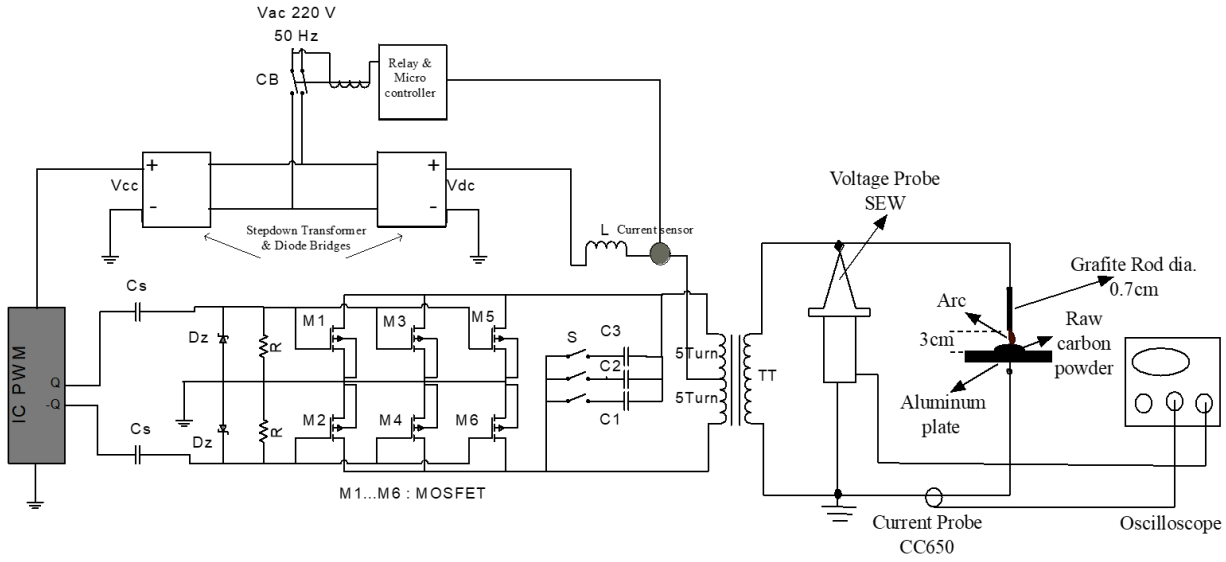

IC PWM : CD4047; M1...M6: MOSFET IRFZ44N; L: Inductor (10 mH)
C1...C3 : Capacitors (100 nF, 150 nF, 200 nF) Dz : Zener diode S: Switch
Cs : PWM Capacitor of 100 nF R : Resistor of 100 Ohm

Figure 1 The electrical circuit for high-voltage generation

2.2. Characterizations

The raw coconut-shell-based charcoal powder and the produced graphene were characterized using Raman spectroscopy, transmission electron microscopy (TEM), and X-ray diffraction (XRD). Raman analysis was conducted using a WITec Alpha 300R Raman spectroscope (WITec GmbH, Ulm, Germany). The vibrations of the molecules were excited using a 488-nm wavelength. The Lorentzian fitting was obtained using OriginPro 8.5.1.315 software. TEM investigations were performed on a JEOL JEM 1400 instrument (JEOL, Peabody, MA, USA) at an accelerating voltage of 120 kV. Furthermore, XRD was conducted using a PANAalytical X'pert PROMRDPW3040 equipped with CuKα radiation at 0.154 nm and operating with a step size of 0.01°.

2.3. Molecular Dynamic Simulation

The simulation began with the preparation of one graphene layer composed of 60 carbon atoms (Nakamura and Ito, 2007). Molecular dynamic simulation was performed using Nanoscale Molecular Dynamic Program v 2.9 with CHARMM 27 used as a force field. The modeled system was subjected to simulated gradual heating at a constant temperature and constant volume (number volume temperature from 0 to 300 K over 100 ps). The molecular dynamic simulation was scaled with 50 ns in time for each system, and it was in iso-thermal and iso-baric boundary conditions. The couplings of temperature and pressure were set at 1.0 ps. The sampling process was saved at every 0.1 ps.

3. Results and Discussion

3.1. Charcoal and Plasma

The implementation of high-voltage plasma for charcoal decomposition and the

resulting decomposed charcoal can be seen in Figures 2a and 2b. The high-voltage plasma glows at a high temperature and has a yellowish-orange color. Plasma was applied evenly across the charcoal's surface with a light intensity of 160 to 198 arbitrary unit (a.u), as seen in Figure 2c. The intensity reference of this measurement tool is 1,000 a.u for white color. The discharge current and voltage are presented in Figure 2d. It is indicated that the discharge current and voltage measured by the tools are 34.3 mA and 7.96 kV, respectively. There are several current pulses that occur in the investigation that arise from zero mA to the current's maximum and minimum values in a cycle of waveform. The high-voltage plasma contains ionic gas molecules and radicals like ozone, nitrogen ions, hydrogen ions, oxygen ions, NOx, and free electrons. This plasma can also flake off the charcoal powder to be graphene nanosheets. If this plasma is stressed by the charcoal powder, it will burn the charcoal powder with a gray color (Figure 2b). After several hours, this powder is cooled at room temperature, and its color changes back to black.

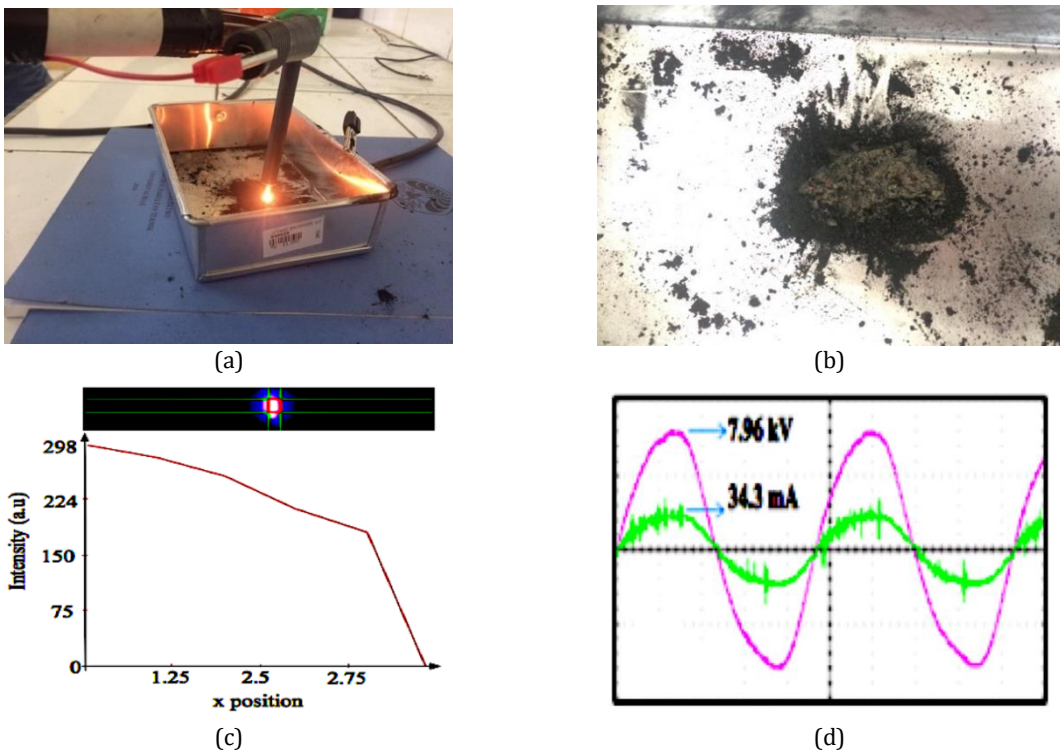

Figure 2 (a) Plasma stressing charcoal; (b)burning charcoal; (c) plasma light intensity; (d) current and voltage

3.2. Raman Spectroscopy Analysis

Figure 3a shows the Raman spectrum of charcoal (raw material) and graphene produced from a high-voltage plasma process at an excitation wavelength of 488 nm. In the Raman spectrum of charcoal in Figure 3a, it can be seen that the presence of two sharp peaks at wavenumbers ~1339.14 cm^{-1} and 1601.16 cm^{-1}, respectively, are known as D band (defect) and G band (graphitic) (Tuinstra and Koenig, 1970; Bokobza et al., 2015). G Band is associated with bond stretching of all sp^2 pairs of carbon atom hybridization, and D band is associated with a scattering process consisting of scattering from crystal defects and inelastic scattering resulting from phonon absorption or release. G band and D band are characteristic bands generally present in carbon materials (whether carbon has a specific graphical sequence or not) (Bokobza et al., 2015). The Raman spectrum of graphene produced in this study (Figure 3a) shows a shift in the peak position of D band (~1364.21

cm^{-1}) and G band (~1598.89 cm^{-1}), as well as the emergence of a more significant additional peak in the wavenumber range of ~2746.09 cm^{-1} (peak in the 2D band area). These peaks are characteristic peaks for graphene materials at an excitation wavelength of 488 nm (Ferrari et al., 2006; Park et al., 2009; Marcus et al., 2010). These results indicate that graphene has been successfully synthesized from charcoal using a high-voltage plasma process.

A 2D band is a band that arises from the second-order Raman scattering process, which involves a double resonance process between the non-equivalent point K in the graphene's first Brillouin zone (Malard et al., 2009). As with D band, the shape and position of the 2D band are very dependent on the excitation laser frequency used (Wall, 2011). The shape and position of this 2D band can be used to identify the number of graphene layers produced. Figure 3a shows that the 2D band of graphene has a broad peak shape (modulated bump) with an intensity ratio of the 2D band and G band of 0.1748 (I_{2D} / I_G = 0.1748). This indicates that the resulting graphene consists of several layers with several defects (Fatima et al., 2014).

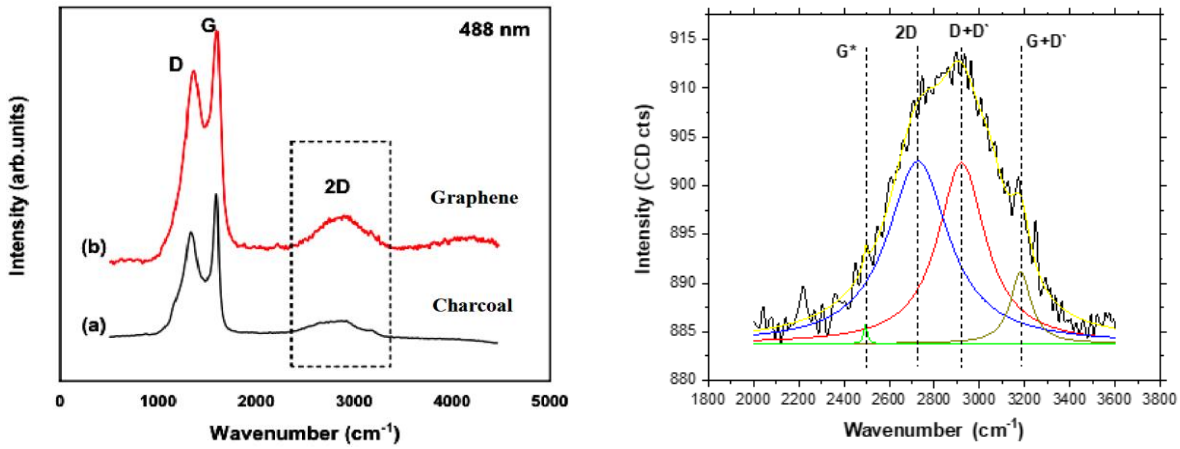

Figure 3 (a) Raman spectrum at 488 nm excitation wavelength; (b) Lorentzian fitting for peaks in the 2D band area of the Raman graphene spectrum

Figure 3b shows the Lorentzian fitting for the peak in the 2D band area of the graphene Raman spectrum. The graph in Figure 3b shows that after the Lorentzian fitting, four Lorentzian peaks are seen that are suitable for the area around the 2D band, namely the wavenumbers ~2492.70 cm^{-1}, ~2723.54 cm^{-1}, ~2925.34 cm^{-1}, and ~3179.73 cm^{-1}, where these peaks are known as the G* band, 2D band, D+D' band, and G+D' band, respectively (Ferrari et al., 2006; Cançado et al., 2008; Malard et al., 2009; Adarsh et al., 2010; Marcus et al., 2010;). These peaks then expand on the resulting graphene spectrum to form a bump-like region. A low 2D band intensity and the shape of a broad peak (bump-like region) consisting of four Lorentzian peaks in the 2D band region in the Raman spectrum of produced graphene have high similarities to the Raman spectrum of FLwG, which has been previously reported by researchers (Manoj and Jerin, 2013; Manoj, 2015). Therefore, it can be concluded that the graphene produced in this study is FLwG.

Furthermore, the quality of the graphene produced can be determined using the intensity ratio of D band and G band (I_D/I_G) (Rogalski et al., 2017). In this study, the Raman spectrum of graphene samples produced by high-voltage plasma processes has an I_D/I_G ratio of 0.8397, while charcoal as a raw material has an I_D/I_G ratio of 0.7426. These results indicate that the resulting graphene and the charcoal have a relatively high number of

defects. Therefore, it can be estimated that the resulting graphene's high defects can come from the fraction of amorphous carbon found in the charcoal. The high temperature produced during the high-voltage plasma process causes several structural defects in the graphene.

3.3. TEM Analysis

The results of the TEM analysis for charcoal and the graphene produced from the high-voltage plasma process are shown in Figure 4. It can be seen that the structure of the charcoal (Figures 4a and 4b) changes after being subjected to the stress plasma process (Figures 4c and 4d). This process produces a material with a thinner structure. It is transparent to the incident electron beam (Figures 4c and 4d) and is similar in structure to graphene material structure (Min and Zhigang, 2015). These results confirm the presence of graphene after a high-voltage plasma process. Furthermore, Figures 4c and 4d also show that the graphene produced has a wrinkled and folded structure. These structures are characteristic of FLwG, which indicates that graphene produced from this process is classified as FLwG (Kaniyoor and Ramaprabhu, 2012). These results are in remarkably good agreement with the Raman spectroscopy analysis. The wrinkles formed due to the folding and twisting of the few-layer graphene sheets, causing deviation from the sp^2/planar characteristic expected for graphene (Kaniyoor and Ramaprabhu, 2012). Deng and Berry (2016) reported that wrinkles and folded structures in graphene influence its electronic properties. The periodic wrinkles or folds in graphene will possess enhanced spin-orbit interaction via curvature, opening gaps, and allowing spin-polarized transport at low magnetic fields (Deng and Berry, 2016).

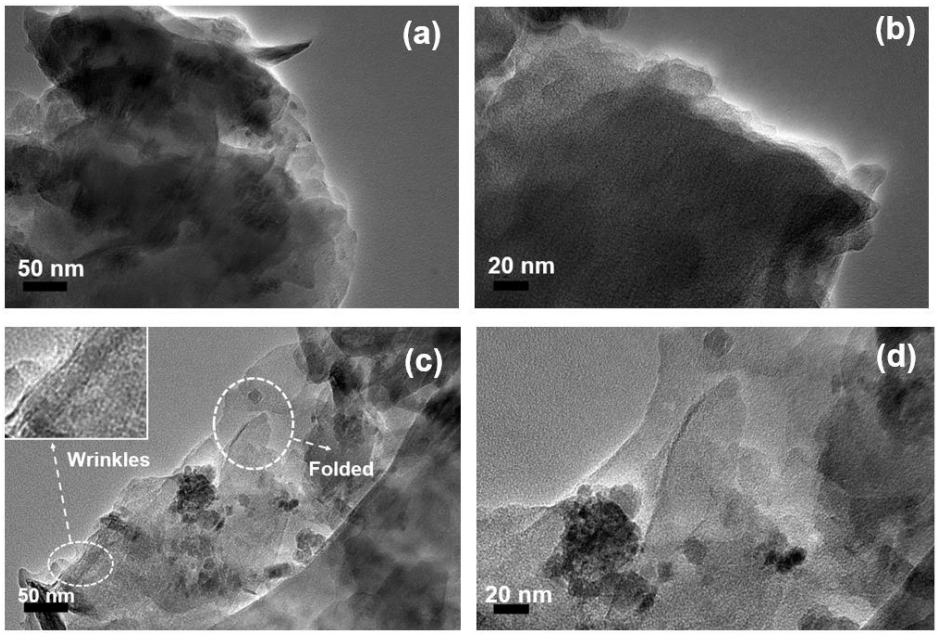

Figure 4 TEM images of (a) and (b) charcoal (raw material) at scale bar of 50 nm and 20 nm, respectively, and (c) and (d) graphene produced from the high-voltage plasma process at scale bar of 50 nm and 20 nm

3.4. XRD Analysis

The XRD spectrum of the charcoal and the graphene are presented in Figure 5a. It can be seen that the XRD spectrum of the charcoal is dominated by the presence of quartz and cristobalite crystalline phases; this crystal phase is the main crystal phase commonly found in charcoal (Phonphuak and Chindaprasirt, 2014). Furthermore, it can be seen that there is

a change in the XRD spectrum of the charcoal after it is stressed by a high-voltage plasma process. There is a shift and decrease in full-width at half-maximum (FWHM) from sharp peaks present in the XRD spectrum of charcoal and the appearance of new peaks at 2θ around ~28.0° (Figure 5b).

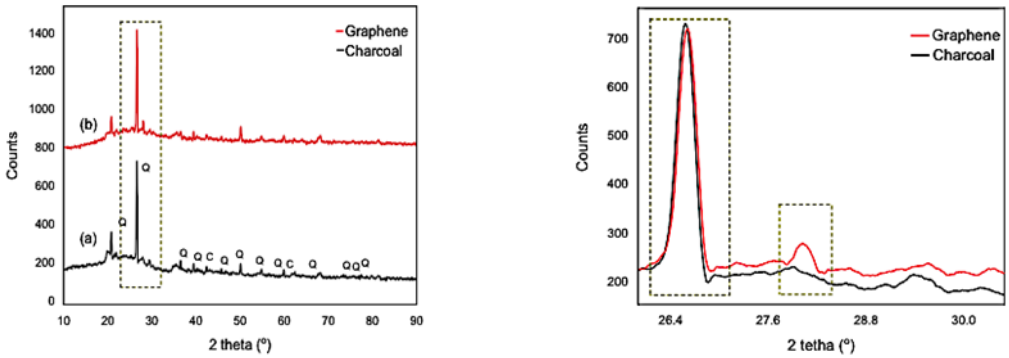

(a) (b)

Figure 5 (a) XRD spectrum, (b) magnification of the XRD spectrum from 26°-30° for charcoal (raw material), and graphene produced from the high-voltage plasma process.

It can be seen that there is a 2θ position shift and a decrease in FWHM at the sharp peaks of charcoal after it is stressed by the high-voltage plasma process. The sharp peak shifts from the 2θ position of 26.6° to 26.7°, and the FWHM decreases from 0.20 to 0.17. According to Poorali and Bagheri-Mohagheghi (2017), the sharp and narrower peak at position 2θ of 26.7° is a characteristic peak for graphene material. The presence of a new peak at the position of 2θ (about ~28.0°) is a graphitic phase peak (Poorali and Bagheri-Mohagheghi, 2017). Furthermore, it is also shown that there are no peaks at positions 2θ of 10°~12°, which indicates there is no formation of graphene oxide (GO) or reduced graphene oxide (rGO) (Kusrini et al., 2019; Hardi and Rahman, 2020). These results indicate that the produced graphene in this study did not undergo any oxidations. Furthermore, the crystal's size for the resulting graphene material can be calculated using the Scherrer equation, as reported by Fadli et al. (2017). The calculations show that the graphene crystal size in this study is 48.03 nm. In general, the difference of physical and chemical properties of graphene, rGO, and GO have been reported (Smith et al., 2019; Taha et al., 2020) and are shown in Table 1.

Table 1 Properties of graphene, GO, and rGO

Properties	Graphene	GO	rGO
Young's modulus	1.0 TPa	207.6±23.4 GPa	250±150 GPa
Thermal conductivity	3000–5000 W m^{-1} K^{-1}	0.5–18 W m^{-1} K^{-1}	1390–2275 W $m^{-1}K^{-1}$
Surface area	2630 m^2 g^{-1}	736.6 m^2 g^{-1}	466–758 m^2 g^{-1}
Electrical conductivity	~6×10^8 S m^{-1}	5.7×10^{-6} S m^{-1}	10^2–10^5 S m^{-1}
Sheet resistance	200 Ω sq^{-1}	~10^{10}–10^{12} Ω sq^{-1}	~10^2–10^6 Ω s^{-1}

The graphene produced from this study was synthesized using a high-voltage plasma process. Plasma is an ionized gas consisting of radicals, positive ions, and negative particles (electrons) in a ratio that makes the overall electric charge equal to zero. In this study, plasma was produced from a high-voltage process that ionized air. The temperature of the plasma has been reported by several previous researchers as being in the range of 400°C-1000°C (Choon et al., 2016). However, according to Laux et al. (2003) the plasma temperature reached >1000°C (Laux et al., 2003). In these temperature ranges, there will be a graphitization process of the charcoal into a structure like graphite (Manoj, 2015).

Because the heating and cooling rates in this process are very fast, they can prevent the buildup of graphene into graphite. Based on the results of the Raman, TEM, and XRD analyses, the produced graphene in this study has a wrinkles and a folded structure, which may be due to the use of high temperatures, resulting in several structural defects in the graphene produced (Botas et al., 2013).

3.5. Molecular Dynamics Results

Graphene was formed by interactions of hydro-carbon and caused the expansion of carbon. Computer simulation through molecular dynamics is needed to study the mechanism and interaction of hydro-carbon. In this study, molecular dynamics can be used to obtain the chemical reaction between hydrogen and graphene. Generally, there are three types of interactions and mechanisms between hydrogen and graphene (Nakamura and Ito, 2007). They are an absorption process with a range energy value of $E_1 < 5$ eV, a reflection process with a range energy value of 5 eV $< E_1 <$ 50 eV, and a penetration process with a range energy value of $E_1 > 50$ eV. Furthermore, if the graphene is absorbed by the hydrogen atom, the nearest carbon atom will be suspended from the graphene. The process of formed graphene is presented in Figure 6.

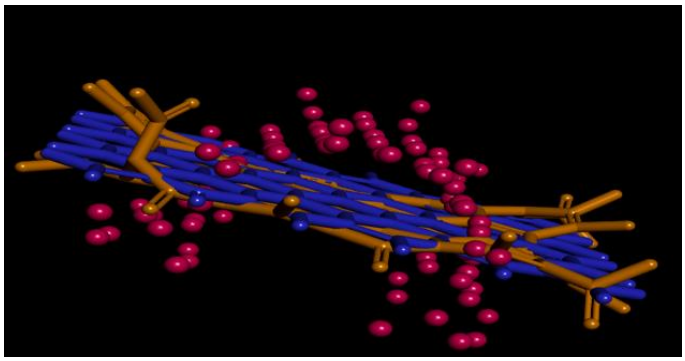

Figure 6 Process of formed graphene. One layer of graphene consisted of 60 carbon atoms (blue). Carbon atoms are suspended (pink); graphene was formed

Molecular dynamics addresses the classical equations of motion for a system of N atoms to generate a conformational search in space or a trajectory under specified thermodynamic conditions (e.g., constant temperature or constant pressure). Molecular dynamic simulation produces some poses. In this study, graphene's best poses were selected with the lowest potential, kinetic energies, and no carbon atom suspension. In this study, the potential energy was obtained at 400 kcal/mol to form stable graphene. The lowest potential energy of molecular dynamic simulation indicates that the molecular system is entirely relaxed and unstrained. This means that all bonds, angles, and torsions are at their "natural" values according to the input force field parameters (Liu et al., 2019). In this study, we performed a molecular dynamics simulation with iso-thermal and iso-baric conditions. It is a proper definition of kinetic energy for controlling the temperature and the pressure of a system.

One of the crucial, fundamental physics concepts is temperature. It was used quantitatively to measure the coldness or hotness of a system. The temperature is also represented by the intensity of the molecule's thermal motion. Molecular dynamics can be used to determine the effect of temperature and the velocity of atoms for control algorithms, as well as to model dynamic processes. There is an urgent need to establish a definition of temperature for non-equilibrium states (Pothoczki et al., 2019; Frimayanti et

al., 2020). A temperature of 300 K is needed to form graphene. When temperature is less than 300 K, the carbon atoms begin to be suspended.

4. Conclusions

This work applied high-voltage plasma generation used to transform charcoal into graphene. The high-voltage electrode was a graphite rod that emitted a large volume of plasma. This plasma also initiated the ionization and deionization processes in an air molecule. Raman spectrophotometry revealed the formation of FLwG. TEM analysis confirmed the presence of FLwG with a wrinkled and folded structure with an average size of 48.03 nm. XRD showed that the produced graphene did not undergo any oxidations during the process. Molecular dynamic simulation showed that the graphene formation was mainly led by the combination of ionization and deionization of air molecules under high temperatures and plasma stressing.

Acknowledgements

We would like to thank Lembaga Penelitian dan Pengabdian Kepada Masyarakat (LPPM) Universitas Riau for providing funding through the Penelitian Inovasi dan Percepatan Hilirisasi research grant (contract number: 842/UN.19.5.1.3/PT.01.03/2020).

References

Adarsh, K., Tessy, T., Sundara, R., 2010. Graphene Synthesis via Hydrogen Induced Low Temperature Exfoliation of Graphite Oxide. *Journal of Materials Chemistry*, Volume 20, pp. 8467–8469

Amri, A., Hendri, Y.B., Yin, C.Y., Rahman, M.M., Altarawneh, M., Jiang, Z.T., 2021. Very-Few-Layer Graphene Obtained from Facile Two-Step Shear Exfoliation in Aqueous Solution. *Chemical Engineering Science*, Volume 245, pp. 116848–116861

Arifutzzaman, A., Ismail, A.F., Alam, M.Z., Khan, A.A., Rahman, S., 2019. Investigation of Extraction Yields of Exfoliated Graphene in Deionized Water from Organic Solvents. *International Journal of Technology*, Volume 10(6), pp. 1251–1259

Bokobza, L., Bruneel, J.L., Couzi, M., 2015. Raman Spectra of Carbon-Based Materials (from Graphite to Carbon Black) and of Some Silicone Composites. *Carbon*, Volume 1(1), pp. 77–94

Botas, C., Patricia, Á., Clara, B., Ricardo, S., Marcos, G., Dolores, G., Rodríguez-Reinoso, F., Rosa, M., 2013. Critical Temperatures in the Synthesis of Graphene-Like Materials by Thermal Exfoliation–Reduction of Graphite Oxide. *Carbon*, Volume 52, pp. 476–485

Cançado, L.G., Reina, A., Kong, J., Dresselhaus, M.S., 2008. Geometrical Approach for the Study of G′ Band in the Raman Spectrum of Monolayer Graphene, Bilayer Graphene, and Bulk Graphite. *Physical Review B*, Volume 77(24), pp. 1–9

Choon, M., Brigitte, V., Siang, P., Abdul, R., 2016. Mechanisms of Graphene Fabrication through Plasma-Induced Layer-by-Layer Thinning. *Carbon*, Volume 105, pp. 496-509

Deng, S., Berry, V., 2016. Wrinkled, Rippled and Crumpled Graphene: An Overview of Formation Mechanism, Electronic Properties, and Applications. *Materials Today*, Volume 19(4), pp. 197–212

Fadli, A., Amri, A., Sari, E.O., Iwantono., Adnan, A., 2017. Crystal-Growth Kinetics of Magnetite (Fe_3O_4) Nanoparticles using the Ostwald Ripening Model. *International Journal of Technology*, Volume 8(8), pp. 1445–1454

Fatima, T., Jee, W., Woo, G., 2014. Facile and Safe Graphene Preparation on Solution-Based Platform. *Journal of Industrial and Engineering Chemistry*, Volume 20(5), pp. 2883–

2887

Ferrari, A., Meyer, J., Scardaci, V., Casiraghi, C., Lazzeri, M., Mauri, F., Geim, A., 2006. Raman Spectrum of Graphene and Graphene Layers. *Physical Review Letters*, Volume 97(18), pp. 1–4

Fri, M., Febrizal, U., Amun, A., 2020. The Effect of The Magnetic Field on an Ozone Generator Fed by a Non-Sinusoidal Resonance Inverter. *International Journal on Electrical Engineering and Informatics*, Volume 12(2), pp. 359–372

Frimayanti, N., Yaeghoobi, M., Namavar, H., Ikhtiarudin, I., Afzali, M., 2020. In Silico Studies and Biological Evaluation of Chalcone-Based 1,5-benzothiazepines as New Potential H1N1 Neuraminidase Inhibitors. *Journal of Applied Pharmaceutical Science*, Volume 10(10), pp. 86–94

Hardi, G.W., Rahman, S.F., 2020. Amperometric Detection of Dopamine based on a Graphene Oxide/PEDOT:PSS Composite Electrode. *International Journal of Technology*, Volume 11(5), pp. 974–983

Kaniyoor, A., Baby, T., Ramaprabhu, S., 2010. Graphene Synthesis via Hydrogen Induced Low Temperature Exfoliation of Graphite Oxide. *Journal of Materials Chemistry*, Volume 20, pp. 8467–8469

Kaniyoor, A., Ramaprabhu, S., 2012. A Raman Spectroscopic Investigation of Graphite Oxide Derived Graphene. *AIP Advances*, Volume 2(3), pp. 1–13

Krishnan, R., John, J., Manoj, B., 2013. Raman Spectroscopy Investigation of Camphor Soot: Spectral Analysis and Structural Information. *International Journal of Electrochemical Science*, Volume 8, pp. 9421–9428

Kusrini, E., Suhrowati, A., Usman, A., Degirmenci, D.V., Khalil, M., 2019. Synthesis and Characterization of Graphite Oxide, Graphene Oxide and Reduced Graphene Oxide from Graphite Waste using Modified Hummers's Method and Zinc as Reducing Agent. *International Journal of Technology*, Volume 10(6), pp. 1093–1104

Laux, C., Spence, T., Kruger, K., Zare, R., 2003. Optical Diagnostics of Atmospheric Pressure Air Plasmas. *Plasma Sources Science and Technology*, Volume 12(2), pp. 125–138

Liu, C., Kelley, C., Jakubikova, E., 2019. Molecular Dynamics Simulations on Relaxed Reduced-Dimensional Potential Energy Surfaces. *The Journal of Physical Chemistry A*, Volume 123(45), pp. 4543–4554

Luong, D.X., Bets, K.V., Al., W.E., 2020. Gram-Scale Bottom-Up Flash Graphene Synthesis. *Nature,* Volume 577(7792), pp. 647–651

Malard, L.M., Pimenta, M.A., Dresselhaus, G., Dresselhaus, M.S., 2009. Raman Spectroscopy in Graphene. *Physics Reports*, Volume 473(5-6), pp. 51–87

Manoj, B., 2015. Synthesis and Characterization of Porous, Mixed Phase, Wrinkled, Few Layer Graphene like Nanocarbon from Charcoal. *Russian Journal of Physical Chemistry A*, Volume 89, pp. 2438–2442

Manoj, K., Jerin, J., 2013. Raman Spectroscopy Investigation of Camphor Soot: Spectral Analysis and Structural Information. *International Journal of Electrochemical Science*, Volume 8, pp. 9421–9428

Marcus, F., Marcus, V.O., Stavale, F., Lucchese, M., Rodrigo, B., Capaz, C., Jorio, A., 2010. Evolution of the Raman Spectra from Single-, Few-, and Many-Layer Graphene with Increasing Disorder. *Physical Review B*, Volume 82, pp. 1–9

Min, Y., Zhigang, S., 2015. A Review on Mechanical Exfoliation for the Scalable Production of Graphene. *Journal of Materials Chemistry A*, Volume 3, pp. 11700–11715

Nakamura, H., Ito, A., 2007. Molecular Dynamics Simulation of Sputtering Process of Hydrogen and Graphene Sheets. *Molecular Simulation*, Volume 33(1-2), pp. 121–126

Park, J.S., Reina, A., Saito, J.K., 2009. G′ Band Raman Spectra of Single, Double and Triple

Layer Graphene. *Carbon*, Volume 47(5), pp. 1303–1310

Phonphuak, N., Chindaprasirt, P., 2014. Types of Waste, Properties, and Durability of Pore-Forming Waste-Based Fired Masonry Bricks. *In:* Eco-Efficient Masonry Bricks and Blocks*.* Elsevier, Amsterdam

Poorali, M., Bagheri-Mohagheghi, M., 2017. Synthesis and Physical Properties of Multi-Layered Graphene Sheets by Arc-Discharge Method with TiO_2 and ZnO Catalytic. *Journal of Materials Science: Materials in Electronics*, Volume 28, pp. 6186–6193

Pothoczki, S., Pusztai, L., Bakó, I., 2019. Molecular Dynamics Simulation Studies of the Temperature-Dependent Structure and Dynamics of Isopropanol–Water Liquid Mixtures at Low Alcohol Content. *The Journal of Physical Chemistry B*, Volume 123(35), pp. 7599–7610

Rogalski, B., Horneber, A., Marius, V. d., Uihlein, J., Heiko, P., Thomas, C., Zhang, D., 2017. STM Tip-Enhanced Raman Spectroscopy and the Investigation of Doped Graphene. *Vibrational Spectroscopy,* Volume 91, pp. 128–135

Smith, A.T., LaChance, A.M., Zeng, S., Liu, B., Sun, L., 2019. Synthesis, Properties, and Applications of Graphene Oxide/Reduced Graphene Oxide and Their Nanocomposites. *Nano Materials Science*, Volume 1(1), pp. 31–47

Tuinstra, F., Koenig, J., 1970. Raman Spectrum of Graphite. *The Journal of Chemical Physics*, Volume 53, pp. 1126–1130

Taha, M.H.F., Ashraf, H., Caesarendra, W., 2020. A Brief Description of Cyclic Voltammetry Transducer-Based Non-Enzymatic Glucose Biosensor using Synthesized Graphene Electrodes. *Applied System Innovation*, Volume 3(3), pp. 1–33

Wall, M., 2011. The Raman Spectroscopy of Graphene and the Determination of Layer Thickness. Available Online at https://tools.thermofisher.com/content/sfs/brochures/AN52252_E%201111%20LayerThkns_H_1.pdf